

Reduced spin Hall effects from magnetic proximity

Wei Zhang, Matthias B. Jungfleisch, Wanjun Jiang, John E. Pearson, and Axel Hoffmann

Materials Science Division, Argonne National Laboratory, Argonne IL 60439, USA

Frank Freimuth and Yuriy Mokrousov

Peter Grunberg Institut and Institute for Advanced Simulation,
Forschungszentrum Julich and JARA, D-52425, Julich, Germany

JUNE 2014

SUBMITTED TO

PHYSICAL REVIEW LETTERS

The submitted manuscript has been created by UChicago Argonne, LLC, Operator of Argonne National Laboratory ("Argonne"). Argonne, a U.S. Department of Energy Office of Science laboratory, is operated under Contract No. DE-AC02-06CH11357. The U.S. Government retains for itself, and others acting on its behalf, a paid-up nonexclusive, irrevocable worldwide license in said article to reproduce, prepare derivative works, distribute copies to the public, and perform publicly and display publicly, by or on behalf of the Government.

Reduced spin Hall effects from magnetic proximity

Wei Zhang,* Matthias B. Jungfleisch, Wanjun Jiang, John E. Pearson, and Axel Hoffmann†
Materials Science Division, Argonne National Laboratory, Argonne IL 60439, USA

Frank Freimuth and Yuriy Mokrousov
*Peter Grünberg Institut and Institute for Advanced Simulation,
 Forschungszentrum Jülich and JARA, D-52425, Jülich, Germany*

(Dated: June 23, 2014)

We investigate temperature-dependent spin pumping and inverse spin Hall effects in thin Pt and Pd in contact with Permalloy. Our experiments show a decrease of the spin Hall effect with decreasing temperature, which is attributed to a temperature-dependent proximity effect. The spin Hall angle decreases from 0.086 at room temperature to 0.042 at 10 K for Pt and is nearly negligible at 10 K for Pd. By first-principle calculations, we show that the spin Hall conductivity indeed reduces by increasing the proximity-induced spin magnetic moments for both Pt and Pd. This work highlights the important role of proximity-induced magnetic ordering to spin Hall phenomena in Pt and Pd.

In metallic conductors with finite spin-orbit coupling, the spin Hall effect (SHE) converts a charge current to a spin current [1, 2]. Conversely the inverse spin Hall effect (ISHE), transforms a spin current into a charge current [3]. The efficiency of this interconversion can be characterized by a single material-specific parameter, the spin Hall angle, γ_{SH} , which is given by the ratio of spin to charge current. Quantification of the spin Hall effect is crucial to the field of spintronics [4, 5]. Experimentally, the spin Hall angle along with other spin transport properties are usually probed via ISHE and injection of a spin current from ferromagnets (FM) to materials with large spin-orbit coupling, usually normal metals (NM), using non-local spin valves [6, 7], ferromagnetic resonance (spin pumping) [8–12], or temperature gradients (spin-Seebeck effect) [13–15]. To maximize the spin Hall signal, the thickness of the NM used in most experiments exceeds the spin diffusion length, λ_{sf} , of the NM. However, when a thin NM (thickness below λ_{sf}) is placed in contact with a FM, interface effects, such as the spin-memory loss [11, 16] and the magnetic proximity effect [17–19] can become significant and alter the spin transport properties of the sample. Of the materials studied for large spin Hall effects, Pt and Pd are two of the most popular metals employed, especially Pt, which has been indispensable in the establishment of virtually all the newly discovered pure spin current phenomena [3, 4, 7–14]. Recently, it has been argued that the proximity effects of Pt and Pd are relevant to many magnetotransport characteristics [20–24], however, their influence on spin Hall effects has not been reported.

In this work, we experimentally study the temperature-dependent evolution of spin Hall effect in Permalloy (Py, Ni₈₀Fe₂₀)/NM bilayers (NM = Pt and Pd) using spin pumping and ISHE measurements. In particular, we investigated such effect in thin samples

with NM thicknesses smaller than the spin diffusion length. We observe a decrease of the spin Hall effect with decreasing temperature, which we ascribe to a temperature-dependent magnetic proximity effect. These results address the temperature dependent spin transport properties of Pt and Pd and highlight the importance of proximity-induced magnetic ordering for their spin Hall effects.

We fabricate the devices using our previous recipe [25]. The key samples are thin Pt (0.6 nm) and thin Pd (3 nm) on top of Py layers (15 nm), respectively. The samples are patterned in the shape of a $20 \mu\text{m} \times 2 \text{mm}$ stripe using lithography on Si substrates with 300-nm-thick thermally grown SiO₂. The electrical leads and the coplanar waveguide (CPW) are subsequently fabricated [Fig. 1(a)]. A 80-nm-thick MgO spacer is used to separate the bilayer stack from the CPW. The measuring frequency is kept between 4 and 6 GHz and the *rf* power is 10 mW.

Figure 1(b) and (c) illustrates the *dc* voltages measured at 4 GHz for Py/Pt and Py/Pd at selective temperatures. The signals have superimposed symmetric and antisymmetric Lorentzian components. The antisymmetric component is attributed to the homodyne anisotropic magnetoresistance (AMR) while the symmetric component results from the ISHE. A reduction of the ISHE component with respect to the AMR is observed with decreasing temperature for both Pt and Pd. Since both ISHE and AMR originate from the *rf*-driven magnetization precession, both effects have thus the same *rf*-power dependence and the resultant *dc* voltage is a sum of the two [25, 26]:

$$V_{dc} = W_{ISHE} \cdot V_{ISHE} + (1 - W_{ISHE}) \cdot V_{AMR}, \quad (1)$$

where W_{ISHE} represents the weight of the symmetric component (ISHE). W_{ISHE} can be further expressed in the form of $W_{ISHE} = 1/(1+V_{AMR}/V_{ISHE})$, and according to previous work [25], the ratio of the two components can be written as:

$$\frac{V_{ISHE}}{V_{AMR}} = \frac{\gamma_{SHE} L E f g_{mix} \lambda_{sf}}{R_{CPW} I_{CPW}} \frac{\hbar_{rf} \rho_{FM}}{\frac{\Delta R_{FM}}{R_{FM}} \Delta H t_{FM}} \tanh\left(\frac{t_{NM}}{2\lambda_{sf}}\right). \quad (2)$$

* zwei@anl.gov.

† hoffmann@anl.gov.

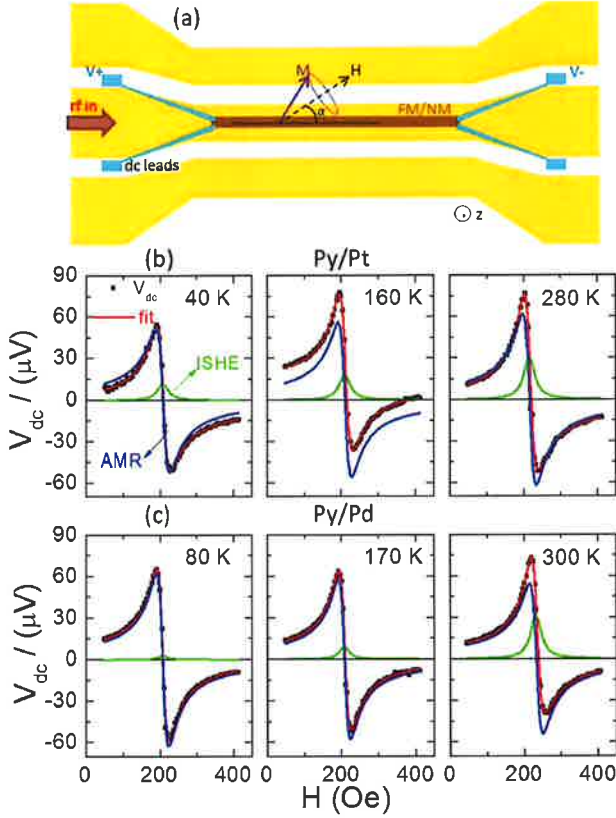


FIG. 1. (Color online) (a) Schematic illustration of the spin pumping and spin Hall effect experiment showing the respective polarity (*rf* input, external field, H , and *dc* voltage contacts, V_+/V_-). The external field direction, $\alpha = 40^\circ$ with respect to the central signal line. AMR-ISHE spectra measured at 4 GHz for (b) Py/Pt and (c) Py/Pd at selective temperatures.

The details of the parameters can be found elsewhere [25]. In Eq. 2, only the spin Hall angle, γ_{SH} , the spin mixing conductance, g_{mix} , and the spin diffusion length, λ_{sf} are dependent on the NM. Therefore, W_{ISHE} can be re-written as:

$$W_{ISHE} = \left(1 + \frac{1}{C \cdot \gamma_{SH} \cdot g_{mix} \cdot \lambda_{sf} \cdot \tanh\left(\frac{t_{NM}}{2\lambda_{sf}}\right)}\right)^{-1}, \quad (3)$$

where C depends only on the characteristics of the CPW as well as the FM layer.

Figure 2 compares the temperature dependence of W_{ISHE} values for Pt and Pd with and without a Cu spacer. The 4 nm Cu spacer in the Py/Cu/NM samples breaks any possible spin interface effect, while only weakly affects the spin current transport due to the long spin diffusion length of Cu [27]. The value of W_{ISHE} strongly decreases with decreasing temperature in Py/NM samples, however, it remains almost independent of temperature for Py/Cu/NM samples. The results for Py/Cu/NM imply a weak temperature dependence

of C as well as the intrinsic spin transport parameters of NMs (γ_{SH} , g_{mix} , and λ_{sf}), which is in agreement with recent experiments using spin Hall magnetoresistance [28]. In contrast to the results for Py/Cu/NM, we attribute the observed strong temperature dependence in Py/NM bilayers to a significant temperature-dependent proximity effect. This magnetic proximity arises at the Py/NM interface and reduces the effective spin Hall angle (which is apparent from the decreasing of the ratio W_{ISHE} with temperature, Fig. 2). Two competing length scales are important in this context: (1) the spin diffusion length of the spin current and (2) the correlation length of the proximity effect, ξ . In our previous studies, we determined the spin diffusion length of Pt (1.2 nm) [25] and Pd (5.5 nm) [26], which is nearly a temperature-independent parameter [25, 28]. However, in these studies we investigated rather thick layers ($t_{NM} > 1$ nm) and it was shown that W_{ISHE} for Pt is almost the same at RT and 10 K. These results imply that the correlation length, which is strongly temperature-dependent [23], is on the order of less than 1 nm for Pt at 10 K, and less than 3 nm for Pd from our present work. Similar values were recently reported for both Pt (0.8 nm) [23] and Pd (2 nm) [24] at low temperatures using different approaches. We conclude that the observed reduction of the spin Hall effect in thin Pt and Pd is due to a temperature-dependent magnetic proximity effect obvious from a strong variation of the ratio ξ/λ_{sf} with temperature.

In order to quantify the temperature-dependent spin Hall angle of the thin Pt and Pd, we distinguish the absolute values of the two voltage components. Figure 3(a) and (e) show the temperature dependence of ISHE and AMR voltages obtained at 4 GHz for Pt and Pd respec-

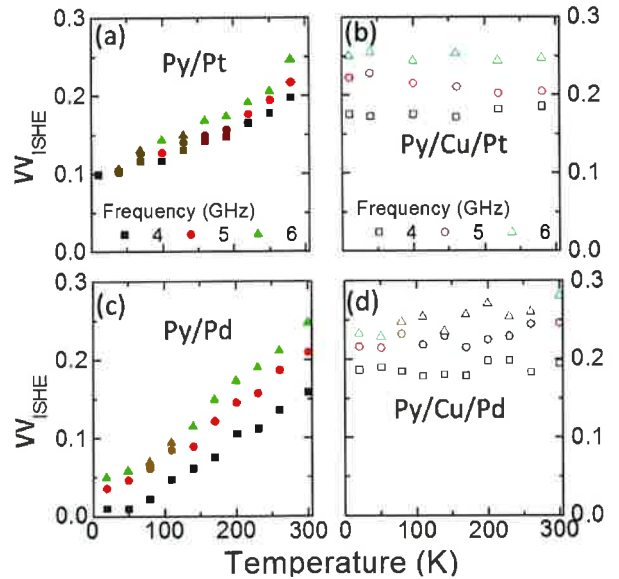


FIG. 2. (Color online) Temperature dependence of W_{ISHE} at 4, 5, and 6 GHz for (a) Py/Pt, (b) Py/Cu/Pt, (c) Py/Pd, and (d) Py/Cu/Pd bilayers.

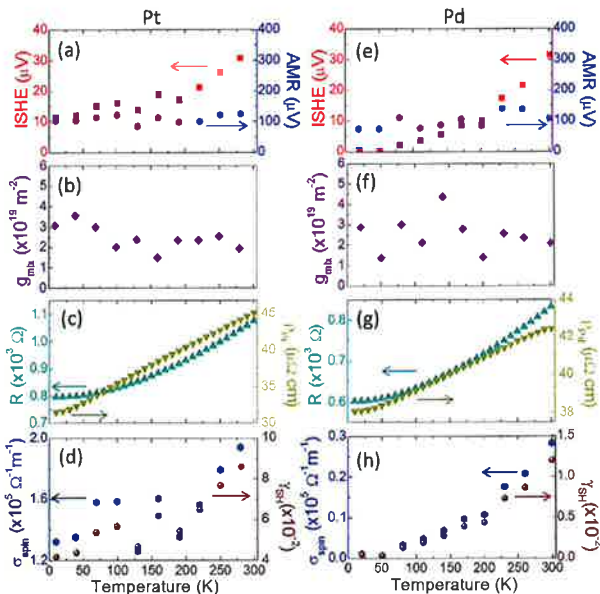


FIG. 3. (Color online) Temperature dependence of (a) AMR and ISHE voltage amplitudes at 4 GHz, (b) spin mixing conductance, (c) device total resistance and resistivity, and (d) calculated spin Hall angle and spin Hall conductivity for Pt. Right panel (e)-(f) are corresponding results for Pd.

tively, which confirm that the decreasing W_{ISHE} is purely due to the decreasing ISHE component. We also extract the effective spin mixing conductance from the damping enhancement due to spin pumping, $\Delta\alpha$ [Fig. 1(b) and (c)], according to [8, 11, 26, 29, 30]:

$$g_{\text{mix}} = \frac{4\pi M_s t_{\text{FM}}}{g\mu_B} \Delta\alpha, \quad (4)$$

where g , μ_B , and M_s are the Landé g factor, Bohr magneton, and saturation magnetization of Py, respectively. We do not observe appreciable temperature dependence of the spin mixing conductance [Fig. 3(b) and (f)]. According to the spin pumping theory [8, 26], the spin Hall angle can be estimated via:

$$V_{\text{ISHE}} = R \cdot \gamma_{\text{SH}} \cdot ewEf g_{\text{mix}} \sin\alpha \sin^2\theta \lambda_{sf} \tanh\left(\frac{t_{\text{NM}}}{2\lambda_{sf}}\right), \quad (5)$$

where w is the width of the stripe and R is the total bilayer resistance. We independently characterize the device resistance and the resistivity of Pt and Pd using four-point measurements in a physical property measurement system (Quantum Design), as illustrated in Fig. 3(c) and (g). Using these values, the spin Hall angles at different temperatures are thus estimated [Fig. 3(d) and (h)] by assuming a temperature-independent precession core-angle, θ , g_{mix} , and λ_{sf} . For Pt, the spin Hall angle decreases from 0.086 at RT [25] to 0.042 at 10 K, i.e., more than a factor of 2; for Pd, we found nearly negligible spin Hall effect at low temperatures as compared to

a spin Hall angle at RT of 0.012 [26]. This result indicates a more significant proximity effect for Pd than for Pt. We also calculate the temperature-dependent spin Hall conductivity σ_{spin} from the relation $\gamma_{\text{SH}} = \sigma_{\text{spin}}/\sigma$, where σ is the electrical conductivity of NMs, $\sigma = \rho^{-1}$. For Pt, the spin Hall conductivity reduces from $(1.9 \pm 0.2) \times 10^5 \Omega^{-1} \text{m}^{-1}$ at RT to $(1.3 \pm 0.2) \times 10^5 \Omega^{-1} \text{m}^{-1}$ at 10 K; for Pd, it is $(0.3 \pm 0.1) \times 10^5 \Omega^{-1} \text{m}^{-1}$ and almost negligible at $T < 80$ K. We note that an opposite trend of γ_{SH} with temperature has been observed for Pd in another report with thicker Pd layers [31], however, such behavior was not reproduced in our samples with the same Pd thickness. An absence of the proximity effect may explain this different temperature dependence.

In order to assess the influence of the proximity induced moment on the SHE, we calculated the spin Hall conductivity of magnetized bulk fcc Pt and Pd from first principles. We determined the electronic structure of paramagnetic Pt and Pd within the generalized gradient approximation to density functional theory [32]. The calculations were performed with the full-potential linearized augmented-plane-wave code FLEUR [33]. In order to minimize the computational cost needed for the computation of the SHE conductivity, we made use of Wannier interpolation [34]. We constructed 18 maximally localized Wannier functions [35, 36] per atom describing the 5s, 4d and 5p states in Pd and the 6s, 5d and 6p states in Pt. Using the electronic structure of the paramagnetic bulk elements represented in the Wan-

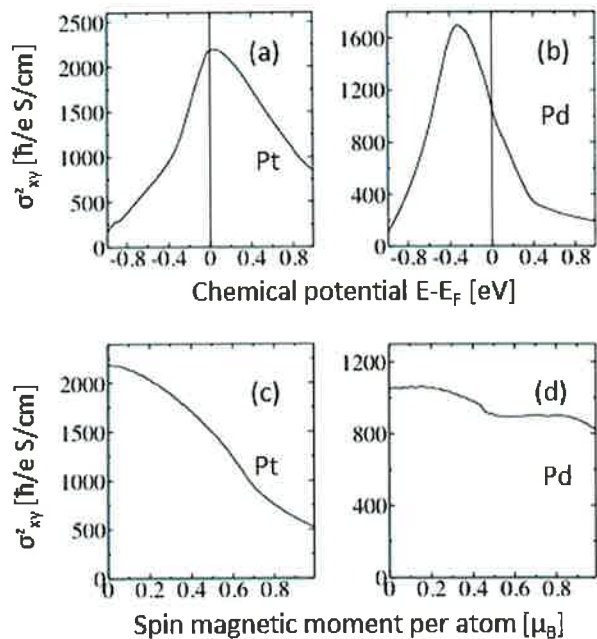


FIG. 4. (a) and (b): Chemical potential dependence of the intrinsic SHE conductivity in Pt and Pd. (c) and (d): Estimated dependence of the intrinsic SHE conductivity on the proximity induced spin magnetic moment.

nier function basis, we evaluated the intrinsic spin Hall conductivity

$$\sigma_{xy}^z(E) = \frac{-2e\hbar}{N} \sum_{E_n < E < E_m} \sum_{\mathbf{k}} \text{Im} \frac{\langle \mathbf{k}n | Q_x^z | \mathbf{k}m \rangle \langle \mathbf{k}n | v_y | \mathbf{k}m \rangle}{(\epsilon_{\mathbf{k}n} - \epsilon_{\mathbf{k}m})^2} \quad (6)$$

as a function of chemical potential E . Here, N is the number of k -points \mathbf{k} , $\epsilon_{\mathbf{k}n}$ is the band energy, v_y is the y component of velocity and $Q_x^z = \frac{\hbar}{4V} [\sigma_z v_x + v_x \sigma_z]$ is the spin current density with V the unit cell volume and σ_z a Pauli matrix. A $800 \times 800 \times 800$ Monkhorst-Pack k -mesh [37] was employed to sample the Brillouin zone. We estimate the SHE conductivity in the presence of a proximity induced spin magnetic moment μ as $\sigma_{xy}^z = [\sigma_{xy}^z(E_\uparrow) + \sigma_{xy}^z(E_\downarrow)]/2$, where E_\uparrow and E_\downarrow are determined from $\mu = n(E_\downarrow) - n(E_\uparrow)$ and $2n(E_F) = n(E_\uparrow) + n(E_\downarrow)$, where $2n(E)$ is the number of states with energy lower than E in the paramagnetic system, and $2n(E_F) = 10$ is the number of valence electrons. In Fig. 4 (a) and (b) we show the SHE conductivity as a function of chemical potential for the paramagnetic case. In the case of Pt, a pronounced maximum is located at $E = E_F$. The chemical potential dependence in Pd is very similar to the Pt case but the maximum is shifted to roughly 0.3 eV below E_F . Figure 4 (c) and (d) show the SHE conductivity in the presence of the induced spin magnetic moment. Due to the maximum of the SHE conductivity at $E = E_F$ in the Pt case shown in (a) the SHE conductivity decreases with increasing moment μ in (c). In contrast, the induced-moment dependence of the SHE in Pd shown in

(d) is much weaker because the maximum of the SHE conductivity in (b) is shifted to 0.3 eV below E_F . Thus for Pt this simple picture with a temperature dependent proximity-induced magnetization may explain quantitatively the observed reduction of the spin Hall effect in Pt. However, the situation in Pd appears to be more complex and may require a more detailed investigation of the interfacial properties.

In summary, we showed the temperature-dependent spin pumping and ISHE effect in thin Pt and Pd layers in contact with Py. We observe a decrease of the spin Hall effect with decreasing temperature, which is attributed to a temperature-dependent proximity effect. By first-principle calculations, we show that the spin Hall conductivity indeed reduces by increasing the proximity-induced spin magnetic moments, and such reduction is predicted to be more pronounced for Pt than Pd. The larger effect for Pd in our experiments remains to be understood by further investigations. This work highlights the important role of proximity-induced magnetic ordering to the spin Hall phenomena of NMs.

This work was supported by the U.S. Department of Energy, Office of Science, Materials Science and Engineering Division. Lithography was carried out at the Center for Nanoscale Materials, which is supported by DOE, Office of Science, Basic Energy Science under Contract No. DE-AC02-06CH11357. Computing time on the supercomputers JUQUEEN and JURIPA at Jülich Supercomputing Center and funding under the HGF-YIG programme VH-NG-513 and SPP 1538 of DFG are gratefully acknowledged.

-
- [1] M. I. D'yakonov and V. I. Perel, *Sov. Phys. JETP Lett.* **13**, 467 (1971).
- [2] J. E. Hirsch, *Phys. Rev. Lett.* **83**, 1834 (1999).
- [3] E. Saitoh, M. Ueda, H. Miyajima, and G. Tatara, *Appl. Phys. Lett.* **88**, 182509 (2006).
- [4] A. Hoffmann, *IEEE Trans. Magn.* **49**, 5172 (2013).
- [5] L. Liu, C. -F. Pai, Y. Li, H. W. Tseng, D. C. Ralph, and R. A. Buhrman, *Science* **336**, 555 (2012).
- [6] S. O. Valenzuela and M. Tinkham, *Nature* **442**, 176 (2006).
- [7] T. Kimura, Y. Otani, T. Sato, S. Takahashi, and S. Maekawa, *Phys. Rev. Lett.* **98**, 156601 (2007).
- [8] O. Mosendz, J. E. Pearson, F. Y. Fradin, G. E. W. Bauer, S. D. Bader, and A. Hoffmann, *Phys. Rev. Lett.* **104**, 046601 (2010).
- [9] F. D. Czeschka, L. Dreher, M. S. Brandt, M. Weiler, M. Althammer, I. Imort, G. Reiss, A. thomas, W. Schoch, W. Limmer, H. Huebl, R. Gross, and S. T. B. Goennenwein, *Phys. Rev. Lett.* **107**, 046601 (2011).
- [10] A. Azevedo, L. H. Vilela-Leão, R. L. Rodríguez-Suárez, A. F. Lacerda Santos, and S. M. Rezende, *Phys. Rev. B* **83**, 144402 (2011).
- [11] J. -C. Rojas-Sanchez, N. Reyren, P. Laczkowski, W. Savero, J. P. Attane, C. Deranlot, M. Jamet, J. -M. George, L. Villa, and H. Jaffres, *Phys. Rev. Lett.* **112**, 106602 (2014).
- [12] H. L. Wang, C. H. Du, Y. Pu, R. Adur, P. C. Hammel, and F. Y. Yang, *Phys. Rev. Lett.* **112**, 197201 (2014).
- [13] K. Uchida, S. Takahashi, K. Harii, J. Ieda, W. Koshibae, K. Ando, S. Maekawa, and E. Saitoh, *Nature* **455**, 778 (2008).
- [14] C. M. Jaworski, J. Yang, S. Mack, D. D. Awschalom, J. P. Heremans, and R. C. Myers, *Nature Mater.* **9**, 898 (2010).
- [15] D. Qu, S. Y. Huang, J. Hu, R. Wu, and C. L. Chien, *Phys. Rev. Lett.* **110**, 067206 (2013).
- [16] H. Kurt, R. Loloee, K. Eid, W. P. Pratt, Jr., and J. Bass, *Appl. Phys. Lett.* **81**, 4787 (2002).
- [17] G. Bergmann, *Phys. Rev. Lett.* **41**, 264 (1978).
- [18] F. Wilhelm, P. Pouloupoulos, G. Ceballos, H. Wende, K. Baberschke, P. Srivastava, D. Benea, H. Ebert, M. Angelakeris, n. K. Flevaris, D. Niarchos, A. Rogalev, and N. B. Brookes, *Phys. Rev. Lett.* **85**, 413 (2000).
- [19] J. Vogel, A. Fontaine, V. Cros, F. Petroff, J. -P. Kappler, G. Krill, A. Rogalev, and J. Goulon, *Phys. Rev. B* **55**, 3663 (1997).
- [20] S. Y. Huang, X. Fan, D. Qu, Y. P. Chen, W. G. Wang, J. Wu, T. Y. Chen, J. Q. Xiao, and C. L. Chien, *Phys. Rev. Lett.* **109**, 107204 (2012).
- [21] Y. Sun, H. Chang, M. Kabatek, Y. -Y. Song, Z. Wang, M. Jantz, W. Schneider, M. Wu, E. Montoya, B. Kardasz, B. Heinrich, S. G. E. te Velthuis, H. Schultheiss, and A.

- Hoffmann, *Phys. Rev. Lett.* **111**, 106601 (2013).
- [22] S. Shimizu, K. S. Takahashi, T. Hatano, M. Kawasaki, Y. Tokura, and Y. Iwasa, *Phys. Rev. Lett.* **111**, 216803 (2013).
- [23] W. L. Lim, N. Ebrahim-Zadeh, J. C. Owens, H. G. E. Hentschel, and S. Urazhdin, *Appl. Phys. Lett.* **102**, 162404 (2013).
- [24] T. Lin, C. Tang, and J. Shi, *Appl. Phys. Lett.* **103**, 132407 (2013).
- [25] W. Zhang, V. Vlaminck, J. E. Pearson, R. Divan, S. D. Bader, and A. Hoffmann, *Appl. Phys. Lett.* **103**, 242414 (2013).
- [26] V. Vlaminck, J. E. Pearson, S. D. Bader, and A. Hoffmann, *Phys. Rev. B* **88**, 064414 (2013).
- [27] T. Wakamura, K. Ohnishi, Y. Niimi, and Y. Otani, *Appl. Phys. Express.* **4**, 063002 (2011).
- [28] S. Meyer, M. Althammer, S. Geprags, M. Opel, R. Gross, and S. T. B. Goennenwein, arXiv preprint: 1401.7787.
- [29] Y. Tserkovnyak, A. Brataas, G. E. W. Bauer, *Phys. Rev. B* **66**, 224403 (2002).
- [30] A. Ghosh, S. Auffret, U. Ebels, and W. E. Bailey, *Phys. Rev. Lett.* **109**, 127202 (2012).
- [31] Z. Tang, Y. Kitamura, E. Shikoh, Y. Ando, T. Shinjo, and M. Shiraishi, *Appl. Phys. Express* **6**, 083001 (2013).
- [32] J. P. Perdew, K. Burke, and M. Ernzerhof, *Phys. Rev. Lett.* **77**, 3865 (1996).
- [33] See <http://www.flapw.de>
- [34] N. Marzari, A. A. Mostofi, J. R. Yates, I. Souza, and D. Vanderbilt, *Rev. Mod. Phys.* **84**, 1419 (2012).
- [35] F. Freimuth, Y. Mokrousov, D. Wortmann, S. Heinze, and S. Blügel, *Phys. Rev. B* **78**, 035120 (2008).
- [36] A. A. Mostofi, J. R. Yates, Y. -S. Lee, I. Souza, D. Vanderbilt, and N. Marzari, *Computer Physics Communications* **178**, 685 (2008).
- [37] H. J. Monkhorst and J. D. Pack, *Phys. Rev. B* **13**, 5188 (1976).